A&A 397, 15–25 (2003)
DOI: 10.1051/0004-6361:20021471

Astronomy & Astrophysics

Analytic calculation of the parallel mean free path of heliospheric cosmic rays

II. Dynamical magnetic slab turbulence and random sweeping slab turbulence with finite wave power at small wavenumbers

A. Teufel and R. Schlickeiser

Institut für Theoretische Physik, Lehrstuhl IV: Weltraum- und Astrophysik, Ruhr-Universität Bochum, 44780 Bochum, Germany

Received 16 August 2002 / Accepted 7 October 2002

Abstract. The parallel mean free path of cosmic ray particles in partially turbulent electromagnetic fields is calculated for two particular turbulence models: slab-like dynamical and random sweeping turbulence. Using the general results for the pitch-angle Fokker-Planck coefficient from Teufel & Schlickeiser (2002) the rigidity dependence and the absolute value of the mean free path for these specific turbulence models are calculated for a turbulence power spectrum with finite wave amplitude at very small wavenumbers. We demonstrate that this modification affects especially the mean free path at very large rigidities. We also derive approximations for the mean free path for realistic Kolmogorov-type turbulence power spectra which include the steepening at high wavenumbers due to turbulence dispersion and/or dissipation.

Key words. cosmic rays – plasmas – turbulence – diffusion – Sun: particle emission

1. Introduction

Besides field line random walk, drifts and non-resonant interactions, resonant wave-particle interaction in the partially random heliospheric magnetic field is regarded as one of the important mechanisms of cosmic ray transport in the heliosphere. In the presence of low-frequency magnetohydrodynamic electromagnetic field fluctuations, the particle's phase space density adjusts rapidly to a quasi-equilibrium through pitch-angle diffusion, which is characterized by a nearly isotropic distribution. The isotropic part of the phase space distribution function $F(\boldsymbol{x}, p, t)$ obeys the diffusion-convection equation including as dominant terms spatial diffusion in the partially irregular magnetic field as well as spatial convection and adiabatic deceleration in the expanding solar wind plasma.

Within quasilinear theory the parallel spatial diffusion coefficient $\kappa_{\|} = \frac{v}{3}\lambda$ and the mean free path λ result from the pitch-angle-cosine ($\mu = p_{\|}/p$) average of the inverse of the pitch-angle Fokker-Planck coefficient $D_{\mu\mu}$ as (Jokipii 1966; Hasselmann & Wibberenz 1968; Earl 1974)

$$\lambda = \frac{3v}{8}\int_{-1}^{1} \mathrm{d}\mu\, \frac{(1-\mu^2)^2}{D_{\mu\mu}(\mu)}. \tag{1}$$

Send offprint requests to: A. Teufel,
e-mail: andreasm4@yahoo.com

The pitch-angle Fokker-Planck coefficient is calculated from the ensemble-averaged first-order corrections to the particle orbits in the weakly turbulent magnetic field (Hall & Sturrock 1968)

$$D_{\mu\mu}(\mu) = Re\int_0^{\infty} \mathrm{d}\xi < \dot{\mu}(t)\dot{\mu}^*(t+\xi) > \tag{2}$$

and depends on the nature and statistical properties of the electromagnetic turbulence and the turbulence-carrying background medium.

Recently (Teufel & Schlickeiser 2002 – hereafter referred to TS) we calculated the parallel mean free path of cosmic ray particles in two particular turbulence models, slab-like dynamical and random sweeping turbulence (Bieber et al. 1994) assuming a turbulence power spectrum with vanishing power below a minimum wavenumber $k_{\min}$. Here we extend our calculations allowing for finite wave amplitudes at large turbulence scales. In Sect. 2 we introduce a flat energy range in the power spectrum and we calculate the new Fokker-Planck coefficient for this modified spectrum. With this new Fokker-Planck coefficient we are able to calculate the mean free path in Sect. 3. In Sect. 4 we show the asymptotic properties of the mean free path and in Sect. 5 we use the very general formulas for the mean free path for special parameters to find new results for high particle rigidities. In Sect. 6 we consider the influence of the dissipation range spectral index.

2. Calculation of the cosmic ray Fokker-Planck coefficient $D_{\mu\mu}$

In TS we derrived the Fokker-Planck-coefficient for two damping models. The first model is called the damping model of dynamical turbulence (hereafter referred to DT) where the damping function is proportional to $\mathrm{e}^{-t/q_\mathrm{D}}$. The second model is called the random sweeping model (hereafter referred to RS) where the damping function is proportional to $\mathrm{e}^{-(t/q_\mathrm{D})^2}$. In TS we demonstrated that the Fokker-Planck-coefficient for the DT-model can be written as

$$D_{\mu\mu}(DT) = \frac{2\pi\Omega^2(1-\mu^2)}{B_0^2}\int_0^\infty \mathrm{d}k_\parallel g(\mid k_\parallel \mid) q_\mathrm{D} \times\left[\frac{1}{1+q_\mathrm{D}^2(k_\parallel v_\parallel-\Omega)^2}+\frac{1}{1+q_\mathrm{D}^2(k_\parallel v_\parallel+\Omega)^2}\right] \quad (3)$$

whereas for the RS-model one obtains

$$D_{\mu\mu}(RS) = \frac{\pi^{3/2}\Omega^2(1-\mu^2)}{B_0^2}\int_0^\infty \mathrm{d}k_\parallel g(\mid k_\parallel \mid) q_\mathrm{D} \times\left[\mathrm{e}^{-(k_\parallel v_\parallel+\Omega)^2 q_\mathrm{D}^2/4}+\mathrm{e}^{-(k_\parallel v_\parallel-\Omega)^2 q_\mathrm{D}^2/4}\right]. \quad (4)$$

Different to TS we use here a flat energy spectrum with finite wave amplitudes below k_min instead of the cut-off at k_min (see Fig. 1):

$$g(k_\parallel)=\begin{cases} g_0 k_\mathrm{min}^{-s} & \text{for} \quad \mid k_\parallel \mid \le k_\mathrm{min} \\ g_0 \mid k_\parallel \mid^{-s} & \text{for} \quad k_\mathrm{min} \le \mid k_\parallel \mid \le k_\mathrm{d} \\ g_1 \mid k_\parallel \mid^{-p} & \text{for} \quad \mid k_\parallel \mid \ge k_\mathrm{d} \end{cases}$$

with $g_1 = g_0 k_\mathrm{d}^{p-s}$, $1<s<2$, $2<p$ and $k_\mathrm{min} \ll k_\mathrm{d}$. g_0 can be expressed in terms of the total fluctuating magnetic field strength:

$$\begin{aligned}(\delta B)^2 &= \sum_{m=1}^{3}(\delta B_\mathrm{m})^2 = \int \mathrm{d}^3k \int \mathrm{d}^3k' \delta B_m(\boldsymbol{k})\delta B_m^*(\boldsymbol{k}')\mathrm{e}^{i(\boldsymbol{k}-\boldsymbol{k}')\boldsymbol{x}} \\ &= \sum_{m=1}^{3}\int \mathrm{d}^3k P_\mathrm{mm}(\boldsymbol{k}) = 8\pi\int_0^\infty \mathrm{d}k_\parallel g(k_\parallel) \\ &= 8\pi g_0\left[\int_0^{k_\mathrm{min}}\mathrm{d}k k_\mathrm{min}^{-s}+\int_{k_\mathrm{min}}^{k_\mathrm{d}}\mathrm{d}k k^{-s}+\frac{g_1}{g_0}\int_{k_\mathrm{d}}^\infty \mathrm{d}k k^{-p}\right] \\ &= \frac{8\pi g_0}{s-1}k_\mathrm{min}^{1-s}\left[s-\left(\frac{k_\mathrm{min}}{k_\mathrm{d}}\right)^{s-1}+\frac{s-1}{p-1}\frac{g_1}{g_0}\frac{k_\mathrm{min}^{s-1}}{k_\mathrm{d}^{p-1}}\right] \\ &\approx \frac{8\pi s g_0}{s-1}k_\mathrm{min}^{1-s}. \end{aligned} \quad (5)$$

With $q_\mathrm{D} = 1/\alpha v_\mathrm{A} \mid k_\parallel \mid$ we derive

$$\begin{aligned}D_{\mu\mu}(DT) &= \frac{(s-1)\Omega^2(1-\mu^2)}{4\alpha s v_\mathrm{A}}\left(\frac{\delta B}{B_0}\right)^2 k_\mathrm{min}^{s-1} \\ &\cdot\left\{k_\mathrm{min}^{-s}\int_0^{k_\mathrm{min}}\mathrm{d}k k^{-1}\left[\frac{1}{1+\left(\frac{k v\mu-\Omega}{\alpha v_\mathrm{A}k}\right)^2}+\frac{1}{1+\left(\frac{k v\mu+\Omega}{\alpha v_\mathrm{A}k}\right)^2}\right]\right. \\ &+\int_{k_\mathrm{min}}^{k_\mathrm{d}}\mathrm{d}k k^{-s-1}\left[\frac{1}{1+\left(\frac{k v\mu-\Omega}{\alpha v_\mathrm{A}k}\right)^2}+\frac{1}{1+\left(\frac{k v\mu+\Omega}{\alpha v_\mathrm{A}k}\right)^2}\right] \\ &\left.+k_\mathrm{d}^{p-s}\int_{k_\mathrm{d}}^\infty \mathrm{d}k k^{-p-1}\left[\frac{1}{1+\left(\frac{k v\mu-\Omega}{\alpha v_\mathrm{A}k}\right)^2}+\frac{1}{1+\left(\frac{k v\mu+\Omega}{\alpha v_\mathrm{A}k}\right)^2}\right]\right\}. \end{aligned} \quad (6)$$

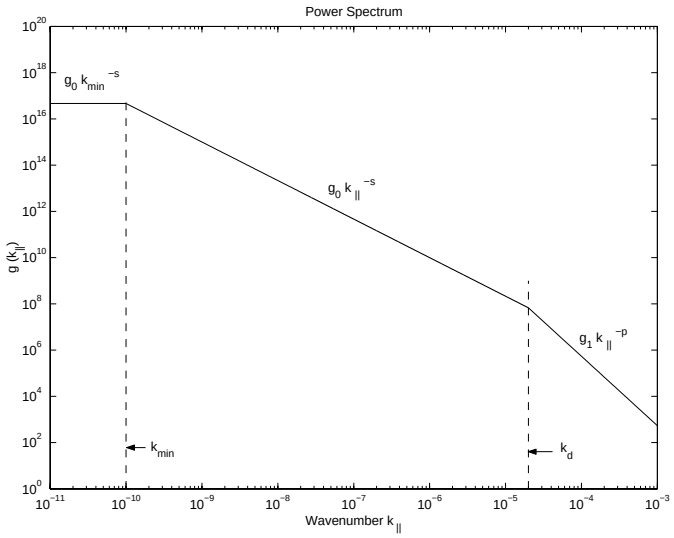

Fig. 1. Power spectrum of slab model used in our calculations.

As in TS it is useful to introduce the following parameters:

$$\begin{aligned}\epsilon &= \frac{v_\mathrm{A}}{v} \\ a &= \frac{1}{\alpha\epsilon} = \frac{v}{\alpha v_\mathrm{A}} \\ b &= \frac{1}{2\alpha\epsilon} = \frac{v}{2\alpha v_\mathrm{A}} = \frac{a}{2} \\ R_\mathrm{L} &= \frac{v}{\Omega} = \frac{pc}{B_0 \mid q \mid} = \frac{r}{B_0} \\ R &= R_\mathrm{L}k_\mathrm{min} = r\frac{k_\mathrm{min}}{B_0} \\ Q &= R_\mathrm{L}k_\mathrm{d} = r\frac{k_\mathrm{d}}{B_0} \end{aligned} \quad (7)$$

with the rigidity $r = pc/\mid q \mid$. Rewriting Eq. (6) as

$$\begin{aligned}D_{\mu\mu}(DT) &= \frac{(s-1)\Omega^2(1-\mu^2)}{4s\alpha v_\mathrm{A}}\left(\frac{\delta B}{B_0}\right)^2 k_\mathrm{min}^{s-1} \\ &\cdot\left\{k_\mathrm{min}^{-s}\int_0^{k_\mathrm{min}}\mathrm{d}k k^{-1}\left[\frac{1}{1+\left(\frac{k v\mu-\Omega}{\alpha v_\mathrm{A}k}\right)^2}+\frac{1}{1+\left(\frac{k v\mu+\Omega}{\alpha v_\mathrm{A}k}\right)^2}\right]\right. \\ &+\int_{k_\mathrm{min}}^{\infty}\mathrm{d}k k^{-s-1}\left[\frac{1}{1+\left(\frac{k v\mu-\Omega}{\alpha v_\mathrm{A}k}\right)^2}+\frac{1}{1+\left(\frac{k v\mu+\Omega}{\alpha v_\mathrm{A}k}\right)^2}\right] \\ &-\int_{k_\mathrm{d}}^{\infty}\mathrm{d}k k^{-s-1}\left[\frac{1}{1+\left(\frac{k v\mu-\Omega}{\alpha v_\mathrm{A}k}\right)^2}+\frac{1}{1+\left(\frac{k v\mu+\Omega}{\alpha v_\mathrm{A}k}\right)^2}\right] \\ &\left.+k_\mathrm{d}^{p-s}\int_{k_\mathrm{d}}^\infty \mathrm{d}k k^{-p-1}\left[\frac{1}{1+\left(\frac{k v\mu-\Omega}{\alpha v_\mathrm{A}k}\right)^2}+\frac{1}{1+\left(\frac{k v\mu+\Omega}{\alpha v_\mathrm{A}k}\right)^2}\right]\right\} \end{aligned} \quad (8)$$

and substituting $x = k_{\rm min}/k$ in the first two integrals and $x = k_{\rm d}/k$ in the last both integrals we find

$$
\begin{aligned}
D_{\mu\mu}(DT) = & \frac{(s-1)v(1-\mu^2)a}{4sk_{\rm min}R_{\rm L}^2}\left(\frac{\delta B}{B_0}\right)^2 \\
& \cdot\left\{\int_1^\infty \frac{{\rm d}x}{x}\left[\frac{1}{1+a^2\,(\mu-x/R)^2}+\frac{1}{1+a^2\,(\mu+x/R)^2}\right]\right. \\
& +\int_0^1 {\rm d}x x^{s-1}\left[\frac{1}{1+a^2\,(\mu-x/R)^2}+\frac{1}{1+a^2\,(\mu+x/R)^2}\right] \\
& -\frac{R^s}{Q^s}\int_0^1 {\rm d}x x^{s-1}\left[\frac{1}{1+a^2\,(\mu-x/Q)^2}+\frac{1}{1+a^2\,(\mu+x/Q)^2}\right] \\
& \left.+\frac{R^s}{Q^s}\int_0^1 {\rm d}x x^{p-1}\left[\frac{1}{1+a^2\,(\mu-x/Q)^2}+\frac{1}{1+a^2\,(\mu+x/Q)^2}\right]\right\}. \qquad (9)
\end{aligned}
$$

Now we do the same calculation for the *RS*-model:

$$
\begin{aligned}
D_{\mu\mu}(RS) = & \frac{\sqrt{\pi}(s-1)\Omega^2(1-\mu^2)}{8\alpha s v_{\rm A}}\left(\frac{\delta B}{B_0}\right)^2 k_{\rm min}^{s-1} \\
& \cdot\left\{k_{\rm min}^{-s}\int_0^{k_{\rm min}} {\rm d}k k^{-1}\left[{\rm e}^{-(k_\parallel v_\parallel-\Omega)^2 q_{\rm D}^2/4}+{\rm e}^{-(k_\parallel v_\parallel+\Omega)^2 q_{\rm D}^2/4}\right]\right. \\
& +\int_{k_{\rm min}}^{k_{\rm d}} {\rm d}k k^{-s-1}\left[{\rm e}^{-(k_\parallel v_\parallel-\Omega)^2 q_{\rm D}^2/4}+{\rm e}^{-(k_\parallel v_\parallel+\Omega)^2 q_{\rm D}^2/4}\right] \\
& \left.+k_{\rm d}^{p-s}\int_{k_d}^\infty {\rm d}k k^{-p-1}\left[{\rm e}^{-(k_\parallel v_\parallel-\Omega)^2 q_{\rm D}^2/4}+{\rm e}^{-(k_\parallel v_\parallel+\Omega)^2 q_{\rm D}^2/4}\right]\right\} \qquad (10)
\end{aligned}
$$

which can be written as

$$
\begin{aligned}
D_{\mu\mu}(RS) = & \frac{\sqrt{\pi}(s-1)v(1-\mu^2)b}{4k_{\rm min}R_L^2}\left(\frac{\delta B}{B_0}\right)^2 \\
& \cdot\left\{\int_1^\infty \frac{{\rm d}x}{x}\left[{\rm e}^{-b^2(\mu-x/R)^2}+{\rm e}^{-b^2(\mu+x/R)^2}\right]\right. \\
& +\int_0^1 {\rm d}x x^{s-1}\left[{\rm e}^{-b^2(\mu-x/R)^2}+{\rm e}^{-b^2(\mu+x/R)^2}\right] \\
& -\frac{R^s}{Q^s}\int_0^1 {\rm d}x x^{s-1}\left[{\rm e}^{-b^2(\mu-x/Q)^2}+{\rm e}^{-b^2(\mu+x/Q)^2}\right] \\
& \left.+\frac{R^s}{Q^s}\int_0^1 {\rm d}x x^{p-1}\left[{\rm e}^{-b^2(\mu-x/Q)^2}+{\rm e}^{-b^2(\mu+x/Q)^2}\right]\right\}. \qquad (11)
\end{aligned}
$$

Note that both expressions (9) and (11) for $D_{\mu\mu}$ do not depend of the charge sign. So we obtain the same λ for electrons and positrons. Moreover, we notice that the $D_{\mu\mu}$ are symmetric functions of μ:

$$
D_{\mu\mu}(-\mu) = D_{\mu\mu}(+\mu). \qquad (12)
$$

2.1. The damping model of dynamical turbulence

Here $D_{\mu\mu}(DT)$ can be written as

$$
D_{\mu\mu}(DT) = \frac{(s-1)v(1-\mu^2)a}{4sk_{\rm min}R_{\rm L}^2}\left(\frac{\delta B}{B_0}\right)^2\cdot I(\mu) \qquad (13)
$$

with

$$
I(\mu) = A + \left(\frac{R}{Q}\right)^s [C-B] + D \qquad (14)
$$

where

$$
\begin{aligned}
A &= \int_0^1 {\rm d}x x^{s-1}\left[\frac{1}{1+a^2\,(\mu-x/R)^2}+\frac{1}{1+a^2\,(\mu+x/R)^2}\right] \\
B &= \int_0^1 {\rm d}x x^{s-1}\left[\frac{1}{1+a^2\,(\mu-x/Q)^2}+\frac{1}{1+a^2\,(\mu+x/Q)^2}\right] \\
C &= \int_0^1 {\rm d}x x^{p-1}\left[\frac{1}{1+a^2\,(\mu-x/Q)^2}+\frac{1}{1+a^2\,(\mu+x/Q)^2}\right] \\
D &= \int_1^\infty \frac{{\rm d}x}{x}\left[\frac{1}{1+a^2\,(\mu-x/R)^2}+\frac{1}{1+a^2\,(\mu+x/R)^2}\right]. \qquad (15)
\end{aligned}
$$

The integrals A, B and C are identical to those in TS and have been approximated there. So here we only have to calculate the integral D. As shown in Appendix A this integral can be solved analytically in different pitch-angle regimes and we obtain approximately

$$
\begin{aligned}
D(\mu R \ll 1, a/R \ll 1) &\approx -2\ln(a/R) \\
D(\mu R \ll 1, a/R \gg 1) &\approx \frac{R^2}{a^2} \\
D(\mu R \gg 1, a\mu \gg 1) &\approx \frac{\pi}{a\mu} \\
D(\mu R \gg 1, a\mu \ll 1) &\approx -2\ln(a/R). \qquad (16)
\end{aligned}
$$

With Eq. (14) and with TS we obtain 9 different cases for I (and therefore 9 different cases for $D_{\mu\mu}$) which are shown in Table 1.

2.2. The random sweeping model

In the *RS*-model $D_{\mu\mu}$ can be written as

$$
D_{\mu\mu}(RS) = \frac{\sqrt{\pi}(s-1)v(1-\mu^2)b}{4sk_{\rm min}R_L^2}\left(\frac{\delta B}{B_0}\right)^2\cdot I(\mu) \qquad (17)
$$

with

$$
I(\mu) = A + \left(\frac{R}{Q}\right)^s [C-B] + D \qquad (18)
$$

where

$$
\begin{aligned}
A &= \int_0^1 {\rm d}x x^{s-1}\left[{\rm e}^{-b^2(\mu-x/R)^2}+{\rm e}^{-b^2(\mu+x/R)^2}\right] \\
B &= \int_0^1 {\rm d}x x^{s-1}\left[{\rm e}^{-b^2(\mu-x/Q)^2}+{\rm e}^{-b^2(\mu+x/Q)^2}\right] \\
C &= \int_0^1 {\rm d}x x^{p-1}\left[{\rm e}^{-b^2(\mu-x/Q)^2}+{\rm e}^{-b^2(\mu+x/Q)^2}\right] \\
D &= \int_1^\infty \frac{{\rm d}x}{x}\left[{\rm e}^{-b^2(\mu-x/R)^2}+{\rm e}^{-b^2(\mu+x/R)^2}\right]. \qquad (19)
\end{aligned}
$$

We solved the integrals A, B and C already in TS. The integral D will be solved by approximations for special cases again. This is done in Appendix B and we obtain

$$
\begin{aligned}
D(\mu R \ll 1, b/R \ll 1) &\approx -\gamma - 2\ln(b/R) \\
D(\mu R \ll 1, b/R \gg 1) &\approx \frac{R^2}{b^2}{\rm e}^{-b^2/R^2} \\
D(\mu R \gg 1, b\mu \gg 1) &\approx \frac{\sqrt{\pi}}{b\mu} \\
D(\mu R \gg 1, b\mu \ll 1) &\approx -\gamma - 2\ln(b/R) \qquad (20)
\end{aligned}
$$

Table 1. This table shows the the function $I(\mu)$ for the DT-model, where we have introduced the functions $f_1(s,p) = \frac{2}{p-2} + \frac{2}{2-s}$ and $f_2(s) = \frac{\pi}{\sin(\frac{\pi s}{2})}$.

Case	$I(\mu)$
$\mu R \gg 1, \mu Q \gg 1, a\mu \ll 1, a/R \ll 1$	$2/s - 2\ln(a/R)$
$\mu R \gg 1, \mu Q \gg 1, a\mu \gg 1$	$\frac{\pi}{a\mu}$
$\mu R \ll 1, \mu Q \gg 1, a\mu \gg 1$	$\pi \frac{R^s}{a} \mu^{s-1}$
$\mu R \ll 1, \mu Q \ll 1, a\mu \gg 1$	$f_1 \frac{R^s Q^{2-s}}{a^2} + \pi \frac{R^s Q^{p-s}}{a} \mu^{p-1}$
$\mu R \ll 1, \mu Q \gg 1, a\mu \ll 1, a/R \gg 1$	$f_2 \frac{R^s}{a^s}$
$\mu R \ll 1, \mu Q \ll 1, a\mu \ll 1, a/R \gg 1, a/Q \gg 1$	$f_1 \frac{R^s Q^{2-s}}{a^2}$
$\mu R \ll 1, \mu Q \ll 1, a\mu \ll 1, a/R \gg 1, a/Q \ll 1$	$f_2 \frac{R^s}{a^s}$
$\mu R \ll 1, \mu Q \gg 1, a\mu \ll 1, a/R \ll 1$	$2/s - 2\ln(a/R)$
$\mu R \ll 1, \mu Q \ll 1, a\mu \ll 1, a/R \ll 1, a/Q \ll 1$	$2/s - 2\ln(a/R)$

Table 2. This table shows the function $I(\mu)$ for the RS-model.

Case	$I(\mu)$
$\mu R \gg 1, \mu Q \gg 1, b\mu \ll 1, b/R \ll 1$	$2/s - \gamma - 2\ln(b/R)$
$\mu R \gg 1, \mu Q \gg 1, b\mu \gg 1$	$\frac{\sqrt{\pi}}{b\mu}$
$\mu R \ll 1, b/R \ll 1, \mu Q \gg 1$	$2/s - \gamma - 2\ln(b/R)$
$\mu R \ll 1, b/R \ll 1, \mu Q \ll 1, b/Q \ll 1$	$2/s - \gamma - 2\ln(b/R)$
$\mu R \ll 1, b/R \gg 1, b\mu \ll 1, \mu Q \gg 1$	$\Gamma(s/2) \frac{R^s}{b^s}$
$\mu R \ll 1, b/R \gg 1, b\mu \ll 1, \mu Q \ll 1, b/Q \ll 1$	$\Gamma(s/2) \frac{R^s}{b^s}$
$\mu R \ll 1, b/R \gg 1, b\mu \ll 1, \mu Q \ll 1, b/Q \gg 1$	$\Gamma(p/2) \frac{Q^{p-s} R^s}{b^p}$
$\mu R \ll 1, b/R \gg 1, b\mu \gg 1, \mu Q \gg 1$	$\sqrt{\pi} \frac{R^s}{b} \mu^{s-1}$
$\mu R \ll 1, b/R \gg 1, b\mu \gg 1, \mu Q \ll 1, b/Q \gg 1$	$\sqrt{\pi} \frac{R^s Q^{p-s}}{b} \mu^{p-1}$

with Euler's constant $\gamma \approx 0.577$. With Eq. (18) and the results from TS we obtain 9 different cases for I (and therefore for $D_{\mu\mu}$) which are shown in Table 2.

3. Equations for the mean free path λ

With the above equations for $D_{\mu\mu}(DT)$ and $D_{\mu\mu}(RS)$ we are able to calculate the parallel mean free path (1).

3.1. Damping model of dynamical turbulence

With Eqs. (1) and (12) we obtain

$$\lambda = \frac{3v}{8} \int_{-1}^{+1} \mathrm{d}\mu \frac{\left(1-\mu^2\right)^2}{D_{\mu\mu}(\mu)} = \frac{3v}{4} \int_0^{+1} \mathrm{d}\mu \frac{\left(1-\mu^2\right)^2}{D_{\mu\mu}(\mu)}. \tag{21}$$

With

$$\lambda_0 = \left(\frac{B_0}{\delta B}\right)^2 \tag{22}$$

and

$$D_{\mu\mu} = \frac{(s-1) k_{\min} a v}{4 s R^2} \left(\frac{\delta B}{B_0}\right)^2 \left(1-\mu^2\right) I(\mu) \tag{23}$$

we derive

$$\frac{\lambda}{\lambda_0} = \frac{3s}{s-1} \frac{R^2}{k_{\min} \cdot a} \cdot K \tag{24}$$

with the integral

$$K = \int_0^1 \mathrm{d}\mu \frac{1-\mu^2}{I(\mu)}. \tag{25}$$

For K we obtain the 12 different cases listed in Table 3. With Eq. (24) these yield the analytical approximations for the mean free path. With the parameters defined in Eq. (7) it is very easy to simplify the results for $1 < s < 2$, $2 < p$ and $R \ll Q$, using approximations like

$$\begin{aligned} K &= \int_0^1 \mathrm{d}\mu \frac{1-\mu^2}{I(\mu)} \\ &\approx \int_0^{1/a} \mathrm{d}\mu \frac{1-\mu^2}{I(a\mu \ll 1)} + \int_{1/a}^1 \mathrm{d}\mu \frac{1-\mu^2}{I(a\mu \gg 1)}. \end{aligned} \tag{26}$$

The first three cases of Table 3 apply to large particle rigidities ($R = R_{\mathrm{L}} k_{\min} \gg 1$). The second three cases are not relevant for typical heliospheric parameters.

3.2. Random sweeping model

For this model we can do similar approximations. But now we have

$$D_{\mu\mu} = \frac{\sqrt{\pi}(s-1) k_{\min} b v}{4 s R^2} \left(\frac{\delta B}{B_0}\right)^2 \left(1-\mu^2\right) I(\mu) \tag{27}$$

so that

$$\frac{\lambda}{\lambda_0} = \frac{3s}{\sqrt{\pi}(s-1)} \frac{R^2}{b k_{\min}} \cdot K \tag{28}$$

Table 3. Analytic expressions for K and therefore the formulas for the mean free path for the DT-model. The functions f_1 and f_2 are defined in Table 1.

Case	K
$1 \ll a \ll R \ll Q$	$\frac{a}{4\pi}$
$1 \ll R \ll Q \ll a$	$\frac{a}{4\pi} + \frac{a^2}{f_1 R^s Q^{3-s}}\ {}_2F_1\left(1, \frac{1}{p-1}, \frac{p}{p-1}, -\frac{\pi a}{f_1 Q}\right)$
$1 \ll R \ll a \ll Q$	$\frac{a}{4\pi}$
$a \ll 1 \ll R \ll Q$	$\frac{s}{3-3s\ln(a/R)}$
$a \ll R \ll Q \ll 1$	$\frac{s}{3-3s\ln(a/R)}$
$a \ll R \ll 1 \ll Q$	$\frac{s}{3-3s\ln(a/R)}$
$R \ll Q \ll 1 \ll a$	$\frac{a^2}{f_1 R^s Q^{2-s}}\left\{ {}_2F_1\left(1, \frac{1}{p-1}, \frac{p}{p-1}, -\frac{\pi a}{f_1} Q^{p-2}\right) - \frac{1}{3}\ {}_2F_1\left(1, \frac{3}{p-1}, \frac{p+2}{p-1}, -\frac{\pi a}{f_1} Q^{p-2}\right)\right\}$
$R \ll Q \ll a \ll 1$	$\frac{2}{3f_1}\frac{a^2}{R^s Q^{2-s}}$
$R \ll 1 \ll a \ll Q$	$\frac{2}{\pi(2-s)(4-s)}\frac{a}{R^s}$
$R \ll 1 \ll Q \ll a$	$\frac{2}{\pi(2-s)(4-s)}\frac{a}{R^s} + \frac{a^2}{f_1 R^s Q^{3-s}}\ {}_2F_1\left(1, \frac{1}{p-1}, \frac{p}{p-1}, -\frac{\pi a}{f_1 Q}\right)$
$R \ll a \ll 1 \ll Q$	$\frac{2}{3f_2}\frac{a^s}{R^s}$
$R \ll a \ll Q \ll 1$	$\frac{2}{3f_2}\frac{a^s}{R^s}$

with the integral

$$K = \int_0^1 \mathrm{d}\mu \frac{1-\mu^2}{I(\mu)}. \tag{29}$$

For K we obtain the 12 cases listed in Table 4, where we have used the same approximations as for the damping model. We can use these approximations for values of $1 < s < 2$, $2 < p$ and $R \ll Q$. The first three cases of Table 3 apply to large particle rigidities ($R = R_{\mathrm{L}} k_{\min} \gg 1$) and the second three cases are not relevant for typical heliosperic parameters again.

4. Asymptotic properties of the mean free path

In this Section we discuss the mean free path for high rigidities $r \to \infty$ and for low rigidities $r \to 0$ for the damping model of dynamical turbulence (DT) and the random sweeping model (RS). We are especially interested in the mean free path at high rigidities which is mostly affected by the finite amplitude power spectrum at small wavenumbers.

4.1. The mean free path for the case of high rigidities $r \to \infty$

We start with the DT-model. In the case of high rigidities we know that

$$a = \frac{1}{\alpha\epsilon} = \frac{c}{\alpha v_{\mathrm{A}}} \frac{r}{\sqrt{r_0^2 + r^2}} \approx \frac{c}{\alpha v_{\mathrm{A}}} \gg 1. \tag{30}$$

With $R \propto r$ and $Q \propto r$ we always have $Q \gg R \gg a \gg 1$. With the results from Table 3 we obtain for this case $K = a/4\pi$. With Eqs. (24) and (22) we find

$$\lambda(DT, r \to \infty) \approx \frac{3 s k_{\min}}{4\pi(s-1)} \frac{r^2}{\delta B^2} \tag{31}$$

where we used a, R and Q from Eq. (7).

Now can do the same calculations for the RS-model. Here we can use

$$b = \frac{1}{2\alpha\epsilon} = \frac{c}{2\alpha v_{\mathrm{A}}} \frac{r}{\sqrt{r_0^2 + r^2}} \approx \frac{c}{2\alpha v_{\mathrm{A}}} \gg 1. \tag{32}$$

With $R \propto r$ and $Q \propto r$ we always have $Q \gg R \gg b \gg 1$. With the results from Table 4 we obtain now $K = b/4\sqrt{\pi}$. With Eqs. (28) and (22) we find

$$\lambda(RS, r \to \infty) \approx \frac{3 s k_{\min}}{4\pi(s-1)} \frac{r^2}{\delta B^2} \tag{33}$$

which is exactly the same result as for the DT-model. So the final result of this subsection is

$$\begin{aligned} \lambda(r \to \infty) &= \lambda(DT, r \to \infty) \\ &= \lambda(RS, r \to \infty) \approx \frac{3 s k_{\min}}{4\pi(s-1)} \frac{r^2}{\delta B^2} \end{aligned} \tag{34}$$

and we notice that the mean free path for high rigidities is only a function of s, $k_{\min}$, δB and r. There is no dependence of k_{d}, p and the background field B_0. It is also important that we have the same mean free path for all particles (electrons, positrons, protons and ions). For the case of high rigidities we also see that the mean free path is always proportional to r^2.

4.2. The mean free path for the case of low rigidities $r \to 0$ and for the DT-model

Now we discuss the mean free path for the case of extremely low rigidities. In this case we have

$$a = \frac{1}{\alpha\epsilon} = \frac{c}{\alpha v_{\mathrm{A}}} \frac{r}{\sqrt{r_0^2 + r^2}} \approx \frac{c}{\alpha v_{\mathrm{A}}} \frac{r}{r_0} \tag{35}$$

for the DT-model. Now we restrict our analysis to

$$\frac{r}{\alpha} \to 0 \tag{36}$$

and

$$r_0 \ll \frac{1}{\alpha} \frac{c}{v_A} \frac{B_0}{k_{\min}} \tag{37}$$

which can be done for realistic physical parameters. We then find always that $1 \gg a \gg R$ and $1 \gg Q \gg R$. So we must discuss the two cases $a \gg Q$ which can be written as $cB_0 \gg \alpha v_{\mathrm{A}} k_{\mathrm{d}} r_0$, and $a \ll Q$ which can be written as $cB_0 \ll \alpha v_{\mathrm{A}} k_{\mathrm{d}} r_0$.

Table 4. Analytic expressions for K and therefore the formulas for the mean free path for the RS-model.

Case	K
$1 \ll b \ll R \ll Q$	$\frac{b}{4\sqrt{\pi}}$
$1 \ll R \ll Q \ll b$	$\frac{b}{4\sqrt{\pi}} + \left[\frac{1}{\Gamma(p/2)} + \frac{1}{\sqrt{\pi}(p-2)}\right] \frac{b^{p-1}}{Q^{p-s}R^s}$
$1 \ll R \ll b \ll Q$	$\frac{b}{4\sqrt{\pi}}$
$b \ll 1 \ll R \ll Q$	$\frac{2}{3} \frac{s}{2-\gamma s-2s\ln(b/R)}$
$b \ll R \ll Q \ll 1$	$\frac{2}{3} \frac{s}{2-\gamma s-2s\ln(b/R)}$
$b \ll R \ll 1 \ll Q$	$\frac{2}{3} \frac{s}{2-\gamma s-2s\ln(b/R)}$
$R \ll Q \ll 1 \ll b$	$\left[\frac{1}{\Gamma(p/2)} + \frac{1}{\sqrt{\pi}(p-2)}\right] \frac{b^{p-1}}{Q^{p-s}R^s}$
$R \ll Q \ll b \ll 1$	$\frac{2}{3\Gamma(p/2)} \frac{b^p}{Q^{p-s}R^s}$
$R \ll 1 \ll b \ll Q$	$\frac{2}{\sqrt{\pi}(2-s)(4-s)} \frac{b}{R^s}$
$R \ll 1 \ll Q \ll b$	$\left[\frac{1}{\Gamma(p/2)} + \frac{1}{\sqrt{\pi}(p-2)}\right] \frac{b^{p-1}}{R^s Q^{p-s}} + \frac{2}{\sqrt{\pi}(2-s)(4-s)} \frac{b}{R^s}$
$R \ll b \ll 1 \ll Q$	$\frac{2}{3\Gamma(s/2)} \frac{b^s}{R^s}$
$R \ll b \ll Q \ll 1$	$\frac{2}{3\Gamma(s/2)} \frac{b^s}{R^s}$

4.2.1. The case $r_0 \ll \frac{cB_0}{\alpha v_A k_d}$

In this case we have $1 \gg a \gg Q \gg R$ and therefore we obtain from Table 3

$$K = \frac{2}{3f_1} \frac{a^2}{R^s Q^{2-s}} \tag{38}$$

and for the mean free path we finally find

$$\lambda(DT, r \to 0, a \gg Q) \approx \frac{2s}{f_1 \cdot (s-1)} \frac{B_0^2}{\delta B^2} \frac{c}{k_{\min} \alpha v_A r_0} \left(\frac{k_{\min}}{k_d}\right)^{2-s} r. \tag{39}$$

We see that the mean free path is linearly proportional to the rigidity. Also we notice that the absolute value of the mean free path is proportional to $1/f_1$ and therefore depends on both turbulence spectral indices p and s,

$$\lambda(DT, r \to 0, a \gg Q) \propto \frac{1}{f_1(s,p)} = \frac{(p-2)(2-s)}{2(p-s)}. \tag{40}$$

For the special parameters of Sect. 5 we find that this case is important for electrons and positrons.

4.2.2. The case $r_0 \gg \frac{cB_0}{\alpha v_A k_d}$

In this case we have $1 \gg Q \gg a \gg R$ and therefore we obtain from Table 3

$$K = \frac{2}{3f_2} \frac{a^s}{R^s} \tag{41}$$

and for the mean free path we finally find

$$\lambda(DT, r \to 0, a \ll Q) \approx \frac{2s}{f_2 \cdot (s-1)} \frac{B_0}{\delta B^2} \left(\frac{cB_0}{\alpha v_A r_0 k_{\min}}\right)^{s-1} r. \tag{42}$$

Again the mean free path is linearly proportional to the rigidity. However, here the mean free path is not a function of the second spectral index p. For the special parameters of Sect. 5 we find that this case is important for protons.

4.3. The mean free path for the case of low rigidities $r \to 0$ and for the RS-model

Now we do the same calculations for the RS-model. Here we have

$$b = \frac{1}{2\alpha\epsilon} = \frac{c}{2\alpha v_A} \frac{r}{\sqrt{r_0^2 + r^2}} \approx \frac{c}{2\alpha v_A} \frac{r}{r_0}. \tag{43}$$

Again, we restrict our analysis to

$$\frac{r}{\alpha} \to 0 \tag{44}$$

and

$$r_0 \ll \frac{1}{2\alpha} \frac{c}{v_A} \frac{B_0}{k_{\min}} \tag{45}$$

implying that we always have $1 \gg b \gg R$ and $1 \gg Q \gg R$. So we must discuss the two cases $b \gg Q$ which can be written as $cB_0 \gg 2\alpha v_A k_d r_0$, and $b \ll Q$ which can be written as $cB_0 \ll 2\alpha v_A k_d r_0$.

4.3.1. The case $r_0 \ll \frac{cB_0}{2\alpha v_A k_d}$

In this case we have $1 \gg b \gg Q \gg R$ and therefore we obtain from Table 4

$$K = \frac{2}{3\Gamma(p/2)} \frac{b^p}{R^s Q^{p-s}} \tag{46}$$

and for the mean free path we finally find

$$\lambda(RS, r \to 0, b \gg Q) \approx \frac{4s}{\sqrt{\pi}(s-1)\Gamma(p/2)} \left(\frac{k_d}{k_{\min}}\right)^s \times \left(\frac{cB_0}{2\alpha v_A r_0 k_d}\right)^p \frac{\alpha v_A r_0 k_{\min}}{\delta B^2 c} r. \tag{47}$$

Like in the DT-model we obtain that the mean free path is linearly proportional to the rigidity. For the special parameters of Sect. 5 we find that this case is important for electrons and positrons.

4.3.2. The case $r_0 \gg \frac{cB_0}{2\alpha v_A k_d}$

In this case we have $1 \gg Q \gg b \gg R$ and therefore we obtain from Table 4

$$K = \frac{2}{3\Gamma(s/2)} \frac{b^s}{R^s} \tag{48}$$

and for the mean free path we finally find

$$\lambda(RS, r \to 0, b \ll Q) \approx \frac{2s}{\sqrt{\pi}\Gamma(s/2)(s-1)} \frac{B_0}{\delta B^2} \left(\frac{cB_0}{2\alpha v_A r_0 k_{\min}} \right)^{s-1} r. \tag{49}$$

From this equation we see that the mean free path is also linearly proportional to the rigidity. Also we notice that the mean free path in this case is not a function of the second spectral index p. For the special parameters of Sect. 5 we find that this case is important for protons.

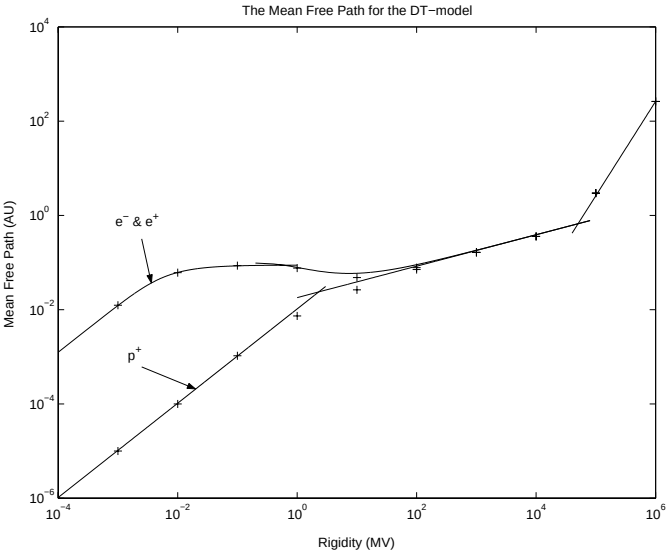

Fig. 2. Parallel mean free paths for electrons, positrons and protons in the damping model of dynamical turbulence. The crosses are the numerical results, the lines are our approximations.

5. Calculating the mean free path for heliospheric parameters

Here we calculate λ for electrons, positrons and protons for typical heliospheric parameters and compare it with numerical solutions to test the approximations we have done. We use the following set of parameters appropriate for interplanetary conditions (Bieber et al. 1994):

$$\begin{aligned} B_0 &= 4.12\,\mathrm{nT} \\ k_{\min} &= 10^{-10}\,\mathrm{m}^{-1} \\ k_d &= 2 \times 10^{-5}\,\mathrm{m}^{-1} \\ s &= 5/3 \\ p &= 3 \\ v_A &= 33.5\,\mathrm{km\,s}^{-1} \\ \alpha &= 1. \end{aligned} \tag{50}$$

With these parameters and with Eq. (7) it is very easy to calculate R, Q, a and b as functions of the rigidity r, and to derive the parallel mean free path for the damping model of dynamical turbulence (using Table 3) and for the random sweeping model (using Table 4).

5.1. Damping model of dynamical turbulence

For protons we obtain three different ranges of λ:

$$\begin{aligned} &\frac{\lambda}{\lambda_0}\left(10^4\ MV \ll r\right) \approx 2.62 \times 10^{-10}\ AU \cdot \left(\frac{r}{MV}\right)^2 \\ &\frac{\lambda}{\lambda_0}\left(10^{-1}\ MV \ll r \ll 10^4\ MV\right) \approx 0.018\ AU \cdot \left(\frac{r}{MV}\right)^{1/3} \\ &\frac{\lambda}{\lambda_0}\left(r \ll 10^{-1}\ MV\right) \approx 0.010\ AU \cdot \left(\frac{r}{MV}\right) \end{aligned} \tag{51}$$

with $r_0 = 938\ MV$. For electrons and positrons we also obtain three ranges:

$$\begin{aligned} &\frac{\lambda}{\lambda_0}\left(10^4\ MV \ll r\right) \approx 2.62 \times 10^{-10}\ AU \cdot \left(\frac{r}{MV}\right)^2 \\ &\frac{\lambda}{\lambda_0}\left(10^{-1}\ MV \ll r \ll 10^4\ MV\right) \approx 0.018\ AU \\ &\cdot \left(\left(\frac{r}{MV}\right)^{1/3} + \frac{3.57}{\left(\left(\frac{r_0}{MV}\right)^2 + \left(\frac{r}{MV}\right)^2\right)^{1/4}} \right) \\ &\frac{\lambda}{\lambda_0}\left(r \ll 10^{-1}\ MV\right) \approx 0.056\ AU \\ &\cdot \left\{ \left[1 + \left(\frac{0.003\ MV}{r} \right)^2 \right] \arctan\left(\frac{r}{0.003\ MV} \right) \frac{0.003\ MV}{r} \right\} \end{aligned} \tag{52}$$

with $r_0 = 0.511\ MV$. Figure 2 shows that the approximations agree very well with the exact numerically integrated results (crosses) for small and medium rigidities.

5.2. Random sweeping model

For protons we obtain three ranges of λ:

$$\begin{aligned} &\frac{\lambda}{\lambda_0}\left(10^4\ MV \ll r\right) \approx 2.62 \times 10^{-10}\ AU \cdot \left(\frac{r}{MV}\right)^2 \\ &\frac{\lambda}{\lambda_0}\left(10^{-1}\ MV \ll r \ll 10^4\ MV\right) \approx 0.018\ AU \cdot \left(\frac{r}{MV}\right)^{1/3} \\ &\frac{\lambda}{\lambda_0}\left(r \ll 10^{-1}\ MV\right) \approx 0.021\ AU \cdot \left(\frac{r}{MV}\right) \end{aligned} \tag{53}$$

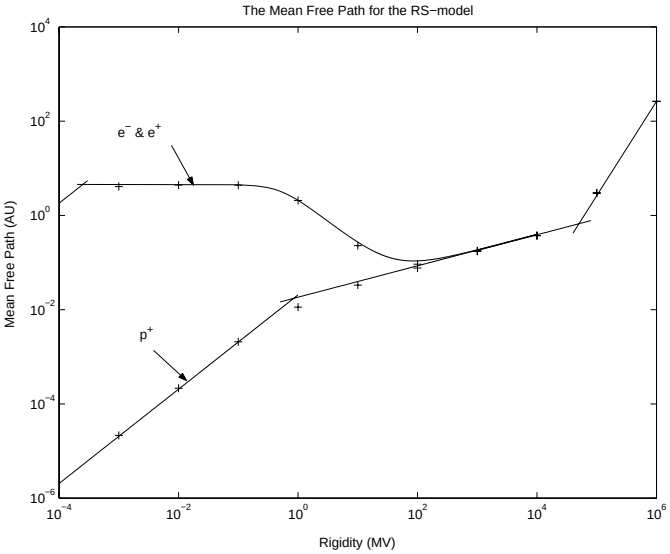

Fig. 3. Parallel mean free paths for electrons, positrons and protons in the random sweeping model. The crosses are the numerical results, the lines are our approximations.

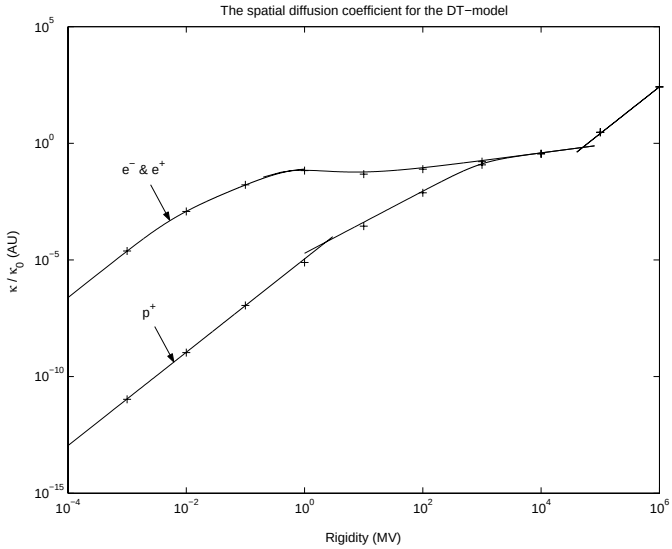

Fig. 4. The parallel spatial diffusion coefficient $\kappa_\parallel$ for the damping model of dynamical turbulence.

with $r_0 = 938\ MV$. For electrons and positrons we also obtain the three ranges:

$$\frac{\lambda}{\lambda_0}\left(10^4\ MV \ll r\right) \approx 2.62 \times 10^{-10}\ AU \cdot \left(\frac{r}{MV}\right)^2$$

$$\frac{\lambda}{\lambda_0}\left(10^{-4}\ MV \ll r \ll 10^4\ MV\right) \approx \frac{2.27\ AU}{\sqrt{\left(\frac{r_0}{MV}\right)^2 + \left(\frac{r}{MV}\right)^2}}$$

$$+0.018\ AU \cdot \left(\frac{r}{MV}\right)^{1/3}$$

$$\frac{\lambda}{\lambda_0}\left(r \ll 10^{-4}\ MV\right) \approx 17.3 \times 10^3 \cdot \left(\frac{r}{MV}\right) \tag{54}$$

with $r_0 = 0.511\ MV$. Figure 3 shows the analytic approximations in comparison with numerical results (crosses) for small, medium and high rigidities. For both models (*DT* and *RS*) we have very good agreement between the approximations and the numerical results for the parallel mean free path.

5.3. The parallel spatial diffusion coefficient

In this section we calculate the parallel spatial diffusion coefficient $\kappa_\parallel$. With the equations for the mean free path and

$$\kappa_\parallel = \frac{v}{3}\lambda \tag{55}$$

we can write the parallel spatial diffusion coefficient as

$$\frac{\kappa_\parallel}{\kappa_0} = \frac{r}{\sqrt{r_0^2 + r^2}}\frac{\lambda}{\lambda_0} \tag{56}$$

with

$$\kappa_0 = \frac{c\lambda_0}{3}. \tag{57}$$

Figures 4 and 5 show $\kappa_\parallel/\kappa_0$ for the *DT*- and the *RS*-model, respectively. If we would adopt as in many previous studies the simple relation $\kappa_\perp = \alpha\kappa_\parallel$ with constant α, Figs. 4 and 5 also show the rigidity dependence of the perpendicular spatial diffusion coefficient for the dynamical turbulence and random sweeping turbulence model.

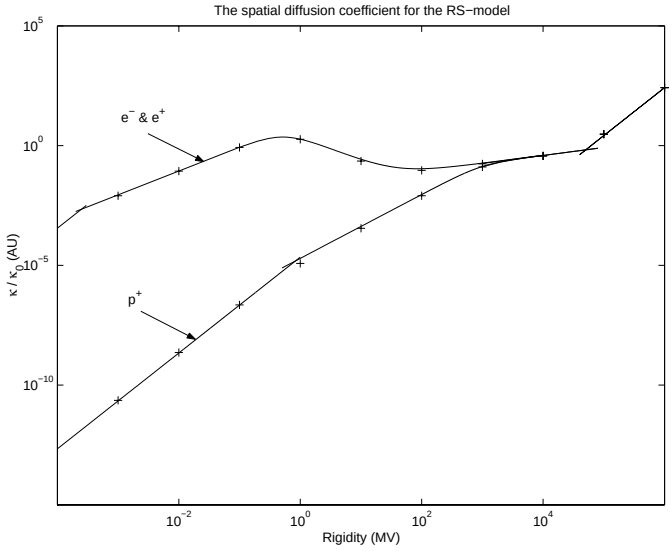

Fig. 5. The parallel spatial diffusion coefficient $\kappa_\parallel$ for the random sweeping model.

6. The mean free path for different values of the dissipation range spectral index p

In the last section we calculated the mean free path for special heliospheric parameters. Because of the limited time resolution of plasma detectors in spacecraft measurements, it is not clear that the dissipation range spectral index p is equal to 3. In this chapter we therefore calculate the mean free path for different values of the dissipative spectral index p. We restrict our analysis to particle rigidities smaller than $10^4\ MV$, because we know

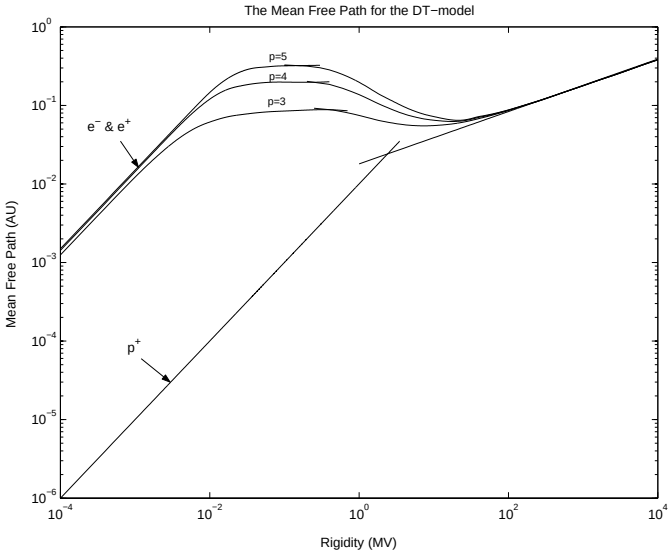

Fig. 6. Parallel mean free paths for electrons, positrons and protons in the damping model for different values of the dissipation range spectral index p.

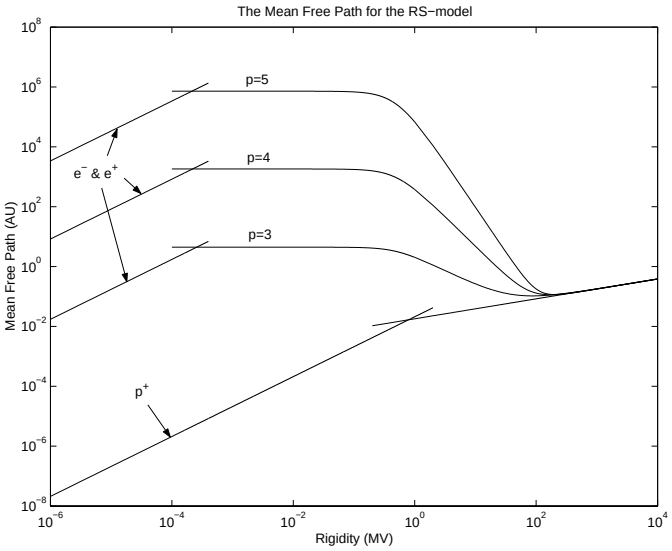

Fig. 7. Parallel mean free paths for electrons, positrons and protons in the random sweeping model for different values of the dissipation range spectral index p.

that for higher rigidities the mean free paths for both damping models (DT and RS) are independent of p (see Eq. (34)).

With Table 3 for the DT-model and Table 4 for the RS-model it is straightforward to calculate the mean free path for different dissipation range spectral indices p. The results are shown in Fig. 6 for the DT-model and Fig. 7 for the RS-model. For both figures we used the parameters of Eq. (50). We notice that there is no p-dependence for protons in both models.

For the DT-model and for electrons and positrons we only find small differences for medium rigidities. For higher rigidities there is no p-dependence and for small rigidities in agreement with our analysis in Sect. 4 we find that the mean free path is proportional to $(p-2)/(p-s)$.

For the RS-model we find that the dependence of p is very strong. For higher values of p and for medium rigidities we find that the value of the mean free path becomes larger than the size of the heliosphere. The fact that the parallel mean free path becomes larger than the dimensions of the heliosphere, may actually not be a problem. Because the magnitude of the perpendicular mean free path is typically only a few percent of the parallel mean free path, the effective radial diffusion coefficient may still be small enough to justify a diffusion approximation.

7. Summary and conclusion

The parallel mean free path of cosmic ray particles in partially turbulent electromagnetic fields is a key input parameter for cosmic ray transport. In this work we have calculated the parallel mean free path of cosmic ray particles in two particular turbulence models: slab-like dynamical and random sweeping turbulence. We extended our earlier calculations by allowing a flat energy range in the power spectrum with finite wave amplitudes at very small wavenumbers. We derive new general formulas for the mean free path (see Tables 3 and 4). These new formulas can also be used for high particle rigidities. We explicitly determine the rigidity dependence and the absolute value of the mean free path for different cosmic ray particles for the DT- and RS-model. In both models the non-zero plasma wave intensity at wavenumbers smaller than $k_{\min}$ yields smaller values of the mean free path at high rigidities as compared to the power spectrum with no wave intensity below $k_{\min}$ considered in TS. We also discuss the influence of the dissipation range spectral index p and the asymptotic properties of the mean free path for both models.

Appendix A: Solving the integral D for the damping model of dynamical turbulence

For the damping model of dynamical turbulence we must solve the integral

$$D = \int_0^\infty \frac{\mathrm{d}x}{x}\left[\frac{1}{1+a^2/R^2\,(\mu R-x)^2}+\frac{1}{1+a^2/R^2\,(\mu R+x)^2}\right]. \tag{A.1}$$

This integral can be solved exactly and we find that

$$D = \frac{1}{1+a^2\mu^2}\left\{\frac{1}{2}\ln\left[(1+\mu R)^2+\frac{R^2}{a^2}\right]+\frac{1}{2}\ln\left[(1-\mu R)^2+\frac{R^2}{a^2}\right] + a\mu\cdot\operatorname{arccot}\left[(1-\mu R)\,\frac{a}{R}\right]-a\mu\cdot\operatorname{arccot}\left[(1+\mu R)\,\frac{a}{R}\right]\right\}. \tag{A.2}$$

While this integral can be solved exactly, for the μ-integration we must employ approximations for special cases.

A.1. The case $\mu R \ll 1$ and $a/R \ll 1$

In the first case we automatically have $a\mu \ll 1$ and we have

$$\begin{aligned} \frac{1}{1+a^2\mu^2} &\approx 1 \\ \ln\left[(1\pm\mu R)^2+\frac{R^2}{a^2}\right] &\approx -2\ln(a/R) \\ \operatorname{arccot}\left[(1\pm\mu R)\frac{a}{R}\right] &\approx \operatorname{arccot}(a/R)\approx\frac{\pi}{2} \end{aligned} \tag{A.3}$$

to find

$$D(\mu R\ll 1, a/R\ll 1)\approx -2\ln(a/R)\,. \tag{A.4}$$

A.2. The case $\mu R \ll 1$ and $a/R \gg 1$

In this case we must approximate the logarithmic function with

$$\ln\left[(1\pm\mu R)^2+\frac{R^2}{a^2}\right]\approx \pm 2\mu R+\frac{R^2}{a^2}-\mu^2R^2 \tag{A.5}$$

and the arccot-function with

$$\operatorname{arccot}\left[(1\pm\mu R)\frac{a}{R}\right]\approx\frac{R}{a}(1\mp\mu R) \tag{A.6}$$

to find finally

$$D(\mu R\ll 1, a/R\gg 1)\approx\frac{R^2}{a^2}\cdot \tag{A.7}$$

A.3. The case $\mu R \gg 1$ and $a\mu \gg 1$

In this case we can use the approximations

$$\begin{aligned} \frac{1}{1+a^2\mu^2} &\approx \frac{1}{a^2\mu^2} \\ \ln\left[(1\pm\mu R)^2+\frac{R^2}{a^2}\right] &\approx 2\ln(\mu R) \\ \operatorname{arccot}\left[(1\pm\mu R)\frac{a}{R}\right] &\approx \operatorname{arccot}(\pm a\mu) \end{aligned} \tag{A.8}$$

to find

$$D(\mu R\gg 1, a\mu\gg 1)\approx\frac{\pi}{a\mu}\cdot \tag{A.9}$$

A.4. The case $\mu R \gg 1$ and $a\mu \ll 1$

In this last case we automatically have $a/R \ll 1$ and we can use

$$\begin{aligned} \frac{1}{1+a^2\mu^2} &\approx 1 \\ \ln\left[(1\pm\mu R)^2+\frac{R^2}{a^2}\right] &\approx -2\ln(a/R) \\ \operatorname{arccot}\left[(1\pm\mu R)\frac{a}{R}\right] &\approx \operatorname{arccot}(\pm a\mu)\approx\frac{\pi}{2} \end{aligned} \tag{A.10}$$

to find

$$D(\mu R\gg 1, a\mu\gg 1)\approx -2\ln(a/R)\,. \tag{A.11}$$

Appendix B: Solving the integral D for the random sweeping model

For the RS-model we must solve the integral

$$D=\int_1^\infty\frac{\mathrm{d}x}{x}\left[\mathrm{e}^{-b^2/R^2[\mu R+x]^2}+\mathrm{e}^{-b^2/R^2[\mu R-x]^2}\right]. \tag{B.1}$$

This integral can not be solved exactly, but we can again employ approximations for four special cases.

B.1. The case $\mu R \ll 1$ and $b/R \ll 1$

In this case we can use $x \gg \mu R$ so that

$$D\approx 2\int_1^\infty\frac{\mathrm{d}x}{x}\mathrm{e}^{-\frac{b^2}{R^2}x^2}=\int_{b^2/R^2}^\infty\frac{\mathrm{d}x}{x}\mathrm{e}^{-x}=E_1\left(b^2/R^2\right) \tag{B.2}$$

where we used the Exponential-Integral-function E_1. In this case $b/R \ll 1$ and we have

$$D(\mu R\ll 1, b/R\ll 1)\approx E_1\left(b^2/R^2\right)\approx -\gamma-2\ln(b/R) \tag{B.3}$$

with Euler's constant $\gamma\approx 0.577$.

B.2. The case $\mu R \ll 1$ and $b/R \gg 1$

In this case we have $b/R \gg 1$ and therefore we find for Eq. (B.2)

$$D(\mu R\ll 1, b/R\gg 1)\approx E_1\left(b^2/R^2\right)\approx\frac{R^2}{b^2}\mathrm{e}^{-b^2/R^2}. \tag{B.4}$$

B.3. The case $\mu R \gg 1$ and $\mu b \gg 1$

In this case we write down the integral D as

$$D=\mathrm{e}^{-b^2\mu^2}\cdot F(\mu b) \tag{B.5}$$

where we introduced the function

$$F(z)=\int_1^\infty\frac{\mathrm{d}x}{x}\left[\mathrm{e}^{+2zxb/R}+\mathrm{e}^{-2zxb/R}\right]\cdot\mathrm{e}^{-\frac{b^2}{R^2}x^2} \tag{B.6}$$

with $z=b\mu$. It is not possible to solve this integral but we know that

$$\begin{aligned} \frac{\mathrm{d}F(z)}{\mathrm{d}z} &= 2\frac{b}{R}\int_1^\infty\mathrm{d}x\left[\mathrm{e}^{+2zxb/R}+\mathrm{e}^{-2zxb/R}\right]\cdot\mathrm{e}^{-\frac{b^2}{R^2}x^2} \\ &= 2\sqrt{\pi}\mathrm{e}^{z^2}\left[\Phi\left(z+\frac{b}{R}\right)-\Phi\left(-z+\frac{b}{R}\right)\right] \end{aligned} \tag{B.7}$$

where we introduced the error function Φ. Now we can use $z=b\mu$ and $\mu R \gg 1$ to obtain

$$\frac{\mathrm{d}F(z)}{\mathrm{d}z}\approx 2\sqrt{\pi}\mathrm{e}^{z^2}\Phi(z) \tag{B.8}$$

where we used $\Phi(z)=-\Phi(-z)$. In this case we have $z=b\mu\gg 1$ and we can use $\Phi(z\gg 1)\approx 1$ to find

$$\frac{\mathrm{d}F(z)}{\mathrm{d}z}\approx 2\sqrt{\pi}\mathrm{e}^{z^2}. \tag{B.9}$$

It is easy to see that

$$F(z)\approx\frac{\sqrt{\pi}}{z}\mathrm{e}^{z^2}+\text{const.}\approx\frac{\sqrt{\pi}}{z}\mathrm{e}^{z^2} \tag{B.10}$$

and we finally find

$$D(\mu R \gg 1, \mu b \gg 1) \approx \frac{\sqrt{\pi}}{\mu b}. \tag{B.11}$$

B.4. The case $\mu R \gg 1$ and $\mu b \ll 1$

In this case we must go back to Eq. (B.8) but now we use $\Phi(z \ll 1) \approx 2z/\sqrt{\pi}$ to find

$$\frac{\mathrm{d}F(z)}{\mathrm{d}z} \approx 4z. \tag{B.12}$$

For the function F we now have

$$F(z) \approx 2z^2 + F(z=0) \approx F(z=0). \tag{B.13}$$

So we obtain for this case

$$D \approx 2\int_1^\infty \frac{\mathrm{d}x}{x} \mathrm{e}^{-\frac{b^2}{R^2}x^2} = \Gamma\left(0, \frac{b^2}{R^2}\right) = E_1\left(\frac{b^2}{R^2}\right). \tag{B.14}$$

In this case we have $b/R \ll 1$ and therefore we find finally

$$D(\mu R \gg 1, \mu b \ll 1) \approx -\gamma - 2\ln(b/R). \tag{B.15}$$

Acknowledgements. We are grateful to the referee, Prof. A. Burger, for his constructive criticism. This work profited enormously from the discussions at the Potchefstroom International Cosmic Ray Workshop in March 2002. AT acknowledges the financial support by the Verbundforschung, grant DESY CH1PCA6. AT and RS acknowledge support by the Deutsche Forschungsgemeinschaft (Schl 201/14-1).

References

Bieber, J. W., Matthaeus, W. H., Smith, C. W., et al. 1994, ApJ, 420, 294
Earl, J. A. 1974, ApJ, 193, 231
Hall, D. E., & Sturrock, P. A. 1967, Phys. Fluids, 10, 2620
Hasselmann, K., & Wibberenz, G. 1968, Z. Geophys., 34, 353
Jokipii, J. R. 1966, ApJ, 146, 480
Teufel, A., & Schlickeiser, R. 2002, A&A, 393, 703 (TS)